

## Inversion of the direction of photo-induced mass transport in $\text{As}_{20}\text{Se}_{80}$ films: Experiment and theory

Yu. Kaganovskii,<sup>1,a)</sup> D. L. Beke,<sup>2</sup> S. Charnovych,<sup>3</sup> S. Kökényesi,<sup>3</sup> and M. L. Trunov<sup>4</sup>

<sup>1</sup>*Department of Physics, Bar-Ilan University, Ramat-Gan 52900, Israel*

<sup>2</sup>*Department of Solid State Physics, University of Debrecen, H-4010 Debrecen, Hungary*

<sup>3</sup>*Department of Experimental Physics, University of Debrecen, H-4010 Debrecen, Hungary*

<sup>4</sup>*Uzhgorod National University, Pidhirna Str., 46 Uzhgorod 88000, Ukraine*

(Received 10 May 2011; accepted 7 August 2011; published online 16 September 2011)

Diffusion mass transfer in thin chalcogenide films under illumination by a focused Gaussian beam have been studied both experimentally and theoretically. It is demonstrated that depending on the light intensity, waist of the beam, and the film thickness, one can obtain formation of either hillocks or dips in the illuminated regions. By comparison of the kinetics of hillock or dip formation on a surface of  $\text{As}_{20}\text{Se}_{80}$  glass films with the results of our theoretical analysis, we have estimated the photo-induced diffusion coefficients,  $D$ , at various light intensities,  $I$ , and found  $D$  to be proportional to  $I$  ( $D = \beta I$ ), with  $\beta \approx 1.5 \times 10^{-18} \text{ m}^4/\text{J}$ . © 2011 American Institute of Physics. [doi:10.1063/1.3636392]

### I. INTRODUCTION

Among various photo-induced physical and chemical processes initiated in chalcogenide glasses (ChGs), such as  $\text{As}_c\text{S}_{1-c}$  or  $\text{As}_c\text{Se}_{1-c}$ , by near bandgap light,<sup>1–9</sup> photo-induced diffusion mass transfer<sup>10–12</sup> is a subject of special scientific and technological interest caused by the possibility of fast optical recording and erasing in ChG films.

Mass transfer was detected under illumination of  $\text{As}_2\text{S}_3$  films by a focused beam of near bandgap light<sup>10</sup> (Argon laser,  $\lambda = 514 \text{ nm}$ ). For incident doses smaller than  $0.6 \text{ kJ/cm}^2$ , hillocks grew on the film surface. In contrast to “giant expansion” of about 2%, (which was previously observed<sup>3</sup> on the  $\text{As}_2\text{S}_3$  surface under sub-bandgap illumination by a focused beam of He–Ne laser), the hillock height under near-bandgap illumination reached about 30% of the film thickness. This means that besides photo-expansion, the hillocks grew because of mass transfer (creep), caused by lateral compressive stresses in the illuminated volume of the film. For doses larger than  $0.6 \text{ kJ/cm}^2$ , a dip instead of hillock was formed in the central illuminated area and pileups at the circumference. Thus, in these experiments, an inversion of the mass transfer direction was observed with the increase of the dose. At small doses, the mass flow was directed toward the maximum of light intensity, whereas at larger doses, the direction of the mass transfer is changed by  $180^\circ$  i.e., the flow was oriented from illuminated regions to dark ones.

The difference in the direction of mass flow was also observed in mass transfer experiments under illumination by two crossed beams, providing periodic intensity distribution. In  $\text{As}_2\text{S}_3$  films, diffraction gratings with sinusoidal surface profile were recorded by Argon laser as a result of mass transfer from bright to dark interference fringes.<sup>10</sup> In con-

trast, in similar experiments on grating formation on  $\text{As}_{0.3}\text{Se}_{0.7}$  films<sup>12</sup> under two-beam illumination by He–Ne laser (near bandgap light for  $\text{As}_{0.3}\text{Se}_{0.7}$ ), the hills grew in the bright interference fringes at the expense of dark fringes where valleys were formed.

It is important that the mass transfer was not induced by thermal effects caused by light absorption; it was basically light-induced mass transfer. As a clear proof, it was found that the direction of the mass transport depended on the direction of light polarization.<sup>10–12</sup>

The above-mentioned inversion of the mass transfer direction in different experiments should be understood and explained. Previously,<sup>13</sup> we have analyzed the kinetics of photo-induced patterning in ChG films, under two-beam illumination by a near-bandgap light, taking into account photo-induced stresses, cleavage of chemical bonds, and capillary forces. It was shown that there is a competition between the diffusion flux induced by stresses and directed toward irradiated regions of the film and the flux induced by an increase of the bulk energy, because of bond cleavage and directed from irradiated to dark regions. As a result, with the variation of the light intensity, one can observe an inversion of the mass transfer direction and thus observe appropriate evolution of the surface profile. Unfortunately, we could not compare our calculations with the experiments carried out at the same film composition and illuminated by light of the same wavelength.

In this paper, we present experimental evidence of the inversion effect in  $\text{As}_{0.2}\text{Se}_{0.8}$  films illuminated by a focused Gaussian beam of He–Ne laser. We calculate the rates of photo-induced variations of surface profile and show that growth of hillocks at low intensities undergoes formation of dips at higher intensities. We introduce the effective photo-induced diffusion coefficient, as a phenomenological coefficient, determining the mass transfer kinetics. It gives the diffusion mobility and thus the drift velocity induced by thermodynamic driving forces (gradients of chemical potential of

<sup>a)</sup>Author to whom correspondence should be addressed. Electronic mail: kagany@biu.ac.il. Fax: 972-3-738-4054.

constituents), in contrast to “ballistic” diffusion coefficient,<sup>14</sup> previously introduced for the description of radiation-induced mixing. Using the photo-induced coefficients as fitting parameters, we compare the calculated and experimental rates of the profile evolution and estimate the photo-induced diffusion coefficients at various light intensities.

## II. EXPERIMENTAL RESULTS

Thin  $\text{As}_{0.2}\text{Se}_{0.8}$  films (1100-nm thick) were prepared by thermal deposition on microscope glass slides in vacuum ( $10^{-5}$ Torr). The material was selected as one of the most efficient for relief recordings among the large number of Se- and S-based glasses.<sup>12,15</sup> Just after the deposition, the films were illuminated by a focused Gaussian beam of a He–Ne polarized laser ( $\lambda = 633$  nm) with the waist of  $w \approx 8$   $\mu\text{m}$  and intensity distribution,

$$I(x) = I_m \exp(-2x^2/w^2). \quad (1)$$

Optical transmission of the films at 633 nm was about 55% corresponding to an absorption coefficient  $\alpha \approx 6 \times 10^3$   $\text{cm}^{-1}$ . After illuminations, the surface profiles were scanned by atomic force microscope (AFM).

Figure 1 shows typical AFM images and appropriate profiles of the film areas illuminated by beams with 32  $\text{W}/\text{cm}^2$  and 320  $\text{W}/\text{cm}^2$  intensities. For 32  $\text{W}/\text{cm}^2$  intensity, convex profile were observed, whereas for 320  $\text{W}/\text{cm}^2$  and higher, concave profiles were observed. The direction of the polarization is also shown in the figure. The anisotropy of the profile is caused by the anisotropy of the mass transfer; parallel to the  $E$ -vector, we observe dips near the hillock [Fig. 1(a)] and hillocks near the dip [Fig. 1(b)], whereas neither dips near the central hillock nor hillocks near the central dip were detected in the perpendicular direction.

Figure 2 shows the dependence of the maximum hillock height (dip depth),  $h_m$ , on the light intensity,  $I_m$ . The  $h_m$  was

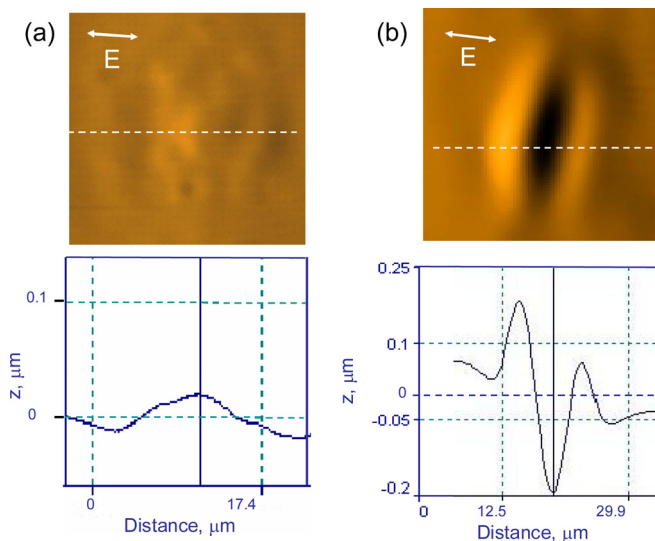


FIG. 1. (Color online) AFM images of hillock (a), and dip (b) obtained after illumination of  $\text{As}_{0.2}\text{Se}_{0.8}$  thin films by focused beam of He–Ne laser. (a)  $I_m = 32$   $\text{W}/\text{cm}^2$ ,  $t = 3 \times 10^4$  s; (b)  $I_m = 320$   $\text{W}/\text{cm}^2$ ,  $t = 3 \times 10^3$  s.

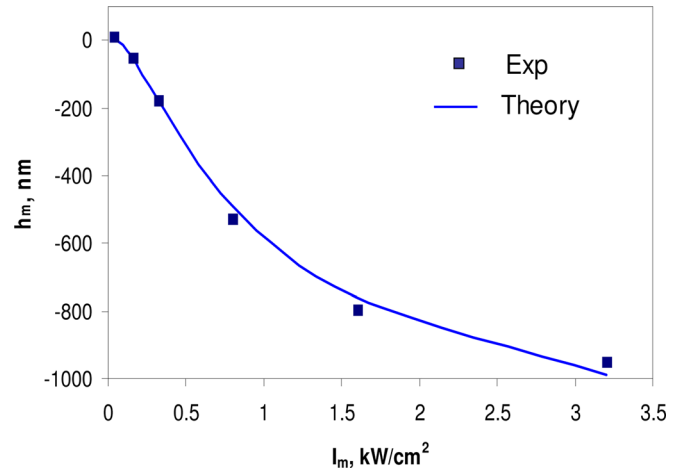


FIG. 2. (Color online) Dependence  $h_m(I_m)$  measured and calculated for  $I_m t = \text{const}$ .

measured in profiles in Fig. 1, as the difference of the heights at  $z = 0$  and  $z$ , which corresponds to the apex of the hillock or dip. With the same irradiation dose,  $I_m t$ , we obtain a variation of  $h_m$  from +10.4 nm at  $I_m = 32$   $\text{W}/\text{cm}^2$  to  $-960$  nm at  $I_m = 3200$   $\text{W}/\text{cm}^2$ .

## III. THEORY

Excitation of ChGs by light with appropriate photon energy,  $\varepsilon_{ph}$ , leads to formation of electron-hole pairs, such as  $P_2^+ - C_1^-$  ( $P$  denotes pnictide atom,  $C$  denotes chalcogen, subscript shows number of bonds, and superscript notes the sign of charge) and accompanies by deformation and breakage of bonds. The  $P_2^+ - C_1^-$  configuration is unstable<sup>1</sup> and it transforms into more stable valence alternation pairs (VAP), also called self-trapped excitons (STE),<sup>1</sup> such as  $P_2^- - C_3^+$ ,  $C_1^- - C_3^+$ ,  $P_2^- - P_4^+$ , or  $C_1^- - P_4^+$ , which can be considered as radiation-induced point defects. Formation of these defects can accelerate atomic jumps and thus results in increase of the diffusion coefficients of both chalcogens and pnictides compared to their thermal diffusion without irradiation.<sup>16</sup>

We consider a ChG film with the thickness  $H$  located on transparent substrate and illuminated by near-bandgap polarized light with the intensity distribution  $I(x)$ ; the  $x$  axis is parallel to the polarization direction.

Following Ref. 13, the chemical potentials of  $P$  and  $C$  atoms can be given as

$$\begin{aligned} \mu_k(x) = & \mu_{0k} + n(x)\omega\varepsilon + \frac{1}{2}\sigma(x)\Delta\omega(x) \\ & + K(x)\gamma\omega(x) - p_k E(x) \quad k = P, C. \end{aligned} \quad (2)$$

Here,  $\mu_{0k}$  is the bulk chemical potential of the atoms in the dark,  $n$  is the number of STE per unit volume,  $\varepsilon$  is the increase of the average bonding energy because of formation of STE,  $\sigma$  is the compressive stress caused by inhomogeneous light-induced volume expansion,<sup>3</sup>  $\omega$  is the average atomic volume,  $\Delta\omega$  is the average volume expansion per atom;  $\omega$ ,  $\Delta\omega$ , and  $\sigma$  are functions of the light intensity and thus functions of  $x$ . The term  $K\gamma\omega$  takes into account capillary forces ( $K\gamma$  is the Laplace pressure) caused by deviation

of the surface profile,  $z(x, t)$ , from the flat one,  $\gamma$  is the surface tension and  $K(x) \approx -z''_{xx}$  is the local surface curvature (for small surface slopes). The last term is just the energy of electric dipole moments,  $p_k$  in the electric field  $E$  induced by the light. The dipole moment  $p_k = \xi_k E$ , where  $\xi_k$  is the electron polarizability. In our previous paper (Ref. 13), we missed the coefficient 1/2 in the third term of Eq. (2) and neglected the last term  $p_k E$ ; this will be justified below. For simplicity of calculations, we assumed that the atomic volumes of  $P$  and  $C$  atoms are equal, as the covalent radii of As and Se are 0.119 and 0.120 nm, respectively.

As it can be seen from Eq. (2), there are several competitive terms, giving different directions of mass transfer. The term  $n(x)\omega\varepsilon$ , describing the increase of  $\mu$  with the light intensity, initiates mass flow from light to dark regions. It competes with the third term,  $\sigma\Delta\omega/2$ , which initiates flow toward the illuminated regions, as well as with the term,  $p_k E$ , which leads to a decrease of  $\mu$  in the illuminated regions (the higher  $E$ , the lower the dipole energy) and thus also initiates flow to the exposed regions. To compare the competitive terms, we have to determine how they depend on the light intensity,  $I$ .

Under continuous wave illumination, the number of transient excitons in steady state,  $n$ , can be estimated from

$$\frac{dn}{dt} = \frac{\alpha \cdot I}{\varepsilon_{ph}} - \frac{n}{\tau} = 0, \quad (3)$$

where  $\alpha$  is the light absorption coefficient,  $I$  is the light intensity,  $\varepsilon_{ph}$  is the photon energy, and  $\tau$  is the average exciton lifetime. The term  $\alpha \cdot I/\varepsilon_{ph}$  gives the number of photons absorbed in unit volume per unit time, which is approximately the number of excited electron-hole pairs transformed into self-trapped excitons. In fact, this term gives the production rate and the second one describes the recombination rate. It follows from Eq. (3) that

$$n = \alpha I \tau / \varepsilon_{ph}. \quad (4)$$

Now the term  $\varepsilon\omega n(x)$  in Eq. (2) can be rewritten as  $qI(x)$  with

$$q \approx \alpha\tau\omega\varepsilon/\varepsilon_{ph}. \quad (5)$$

The coefficient  $q$  depends on the exciton lifetime  $\tau$ , which can be estimated from Eq. (4). With plausible density of STE,<sup>17</sup>  $n \approx 10^{18} \text{ cm}^{-3}$  under illumination by light with  $I \approx 100 \text{ W/cm}^2$ ,  $\varepsilon_{ph} \approx 2 \text{ eV}$ , and  $\alpha \approx 6 \times 10^3 \text{ cm}^{-1}$ , we obtain  $\tau \approx 0.5 \times 10^{-6} \text{ s}$ . It is worth noting that the absorption coefficient  $\alpha$  in Eq. (4) increases with the increase of  $\varepsilon_{ph}$ . However, Eq. (4) does not contain the dependence of  $n$  on the light penetration depth,  $z$ ; for simplicity, we neglect dependence  $n(z)$  as we assumed near-bandgap illumination. With  $\varepsilon_{ph} \gg E_g$  ( $E_g$  is the bandgap energy), when only the subsurface layer of the film is excited, no mass transfer takes place at all.

The third term,  $\sigma\Delta\omega/2$ , takes into account lateral compressive stresses in the film as a result of light-induced giant expansion caused by elongation of the chemical bond and repulsive Coulomb forces between layered clusters.<sup>18</sup> The free expansion is possible in the direction perpendicular to the

sample surfaces, whereas the lateral volume expansion is partly hindered by non-illuminated regions. The stresses induce mass flow toward the illuminated regions on a free surface and relax because of formation of hillocks. The lateral compressive stress,  $\sigma$ , in the circularly illuminated area,  $a = \pi r^2$ , is proportional to  $\Delta a/a = 2\Delta r/r$ , where the relative linear expansion can be given as  $\Delta r/r \approx \Delta\omega/3\omega_0$ . Thus,  $\sigma \approx (2/3)E_Y\Delta\omega/\omega_0$  ( $E_Y$  is the Young's modulus).

As it follows from experimental results,<sup>3</sup> the volume expansion increases with increasing dose; however, there exists a certain maximal deformation,  $e_m$  (saturation of the expansion), depending on the light intensity. One can express the intensity dependence of the expansion in the form (see also Ref. 13)

$$\frac{\Delta\omega}{\omega_0} \approx \frac{\zeta I e_m}{\zeta I + e_m}, \quad e_m = e_0 + b \cdot I, \quad (6)$$

so that at low intensities ( $\zeta I \ll e_m$ ),  $\Delta\omega/\omega_0 \approx \zeta I$ , whereas at high intensities ( $\zeta I \gg e_m$ ),  $\Delta\omega/\omega_0 \approx e_m$ . From the data on photo-induced volume expansion,<sup>3</sup> we estimated  $e_0 \approx 0.01$ ,  $b \approx 9 \times 10^{-6} \text{ cm}^2/\text{W}$ , and  $\zeta \approx 1 \times 10^{-4} \text{ cm}^2/\text{W}$ , and we used these values in our calculations.

The term  $K\gamma\omega$  initiates mass flow from the regions with positive curvature  $K$  toward those with negative  $K$ , independently of the light intensity; this flow flattens both hillocks and dips on the film surface.

Using the formula<sup>19</sup>

$$I = \frac{n_r c}{2\pi} |E^2|, \quad (7)$$

for the intensity associated with the light field  $E$  ( $n_r$  is the refractive index of the film,  $c \approx 3 \times 10^8 \text{ m/s}$  is the speed of light in vacuum), one can compare the terms  $qI$  and  $-p_k E = -(2\pi \xi_k/n_r c)I$  in Eq. (2). Substituting  $\alpha = 6 \times 10^5 \text{ m}^{-1}$ ,  $\varepsilon/\varepsilon_{ph} \approx 0.5$ ,  $\tau \approx 0.5 \mu\text{s}$ , and  $\omega \approx 2 \times 10^{-29} \text{ m}^3$  in Eq. (5), we have  $q \approx 3 \times 10^{-30} \text{ m}^2\text{s}$ . With<sup>20</sup>  $\xi_k \approx 5 \times 10^{-30} \text{ m}^3$  and  $n_r \approx 2.5$ , we obtain  $2\pi \xi_k/n_r c \approx 4.2 \times 10^{-38} \text{ m}^2\text{s}$ , i.e.,  $2\pi \xi_k/n_r c \ll q$  and thus in Eq. (2), we can neglect the term  $p_k E$  compared to  $qI$ .

We consider bulk diffusion as the main mechanism of diffusion flow and neglect the surface diffusion mechanism. Indeed, according to data on spectral dependence of photo-induced viscosity<sup>2</sup> and photo-induced deformation,<sup>21</sup> light with the photon energy higher than the bandgap does not induce mass transfer, although electron-hole pairs would be excited in the subsurface layer and might induce fast surface diffusion.

Light-induced lateral diffusion fluxes of  $P$  and  $C$  atoms in the bulk of the film depend on  $x$  as follows:<sup>13</sup>

$$J_{kx}(x, z) = -\frac{D_{kx}(x)}{kT} N_k \frac{\partial \mu_k(x, z)}{\partial x} \quad k = P, C. \quad (8)$$

Here,  $N_k(x)$  is the number of  $P$  and  $C$  atoms per unit volume of the film, and  $D_{kx}$  is the diffusion coefficient, which we assumed to be proportional to the light intensity:  $D_{kx} = \beta_k I$  ( $k$  denotes  $P$  or  $C$  atoms) in the  $x$ -direction. Besides, there are also stress-induced fluxes in  $z$ -direction, toward a free surface of the film; these fluxes also depend on  $x$ :

$$J_{kz}(x, z) = -\frac{D_{kz}(x)}{kT} N_k \frac{\partial \mu_k(x, z)}{\partial z}. \quad (9)$$

Under illumination by a polarized light with polarization vector parallel to the  $x$  axis, the coefficients  $D_{kz}$  are about one order of magnitude less than  $D_{kx}$ .<sup>11</sup> We assumed  $D_{kz} = D_k/s$  with  $s \approx 5-10$ . Variation of the surface profile can be calculated as<sup>13</sup>

$$\frac{\partial z}{\partial t} = -H \left( \frac{\partial J_{Px}}{\partial x} \omega_P + \frac{\partial J_{Cx}}{\partial x} \omega_C \right) + J_{Pz}(x) \omega_P + J_{Cz}(x) \omega_C. \quad (10)$$

As the film thickness is compared to inverse absorption coefficient, we can assume that the diffusion coefficients  $D_{kx}$  and  $D_{kz}$ , depend only on  $x$ -coordinate. We assume that the stresses relax at the film surface ( $z=H$ ), i.e.,  $\partial \mu_k / \partial z \approx [\mu_k(H) - \mu_k(0)]/H \approx -\sigma \Delta \omega / 2H$ .

Taking into account that all quantities, determining the bulk diffusion flow, depend on the light intensity and thus on the  $x$ -coordinate, we obtained a rather complicated equation for evolution of the surface profile,  $z(x, t)$ , which we solved numerically. The values of parameters used for calculations are presented above. We assumed, similarly as in Ref. 14 for the diffusion in binary system, that the diffusion fluxes of pnictides and chalcogenes are independent of each other and used the effective diffusion coefficient in the polarization direction ( $x$ ) defined by formula

$$D_x = D_{Pc} + D_C(1 - c). \quad (11)$$

This also means that we neglect the segregation caused by the difference of pnictide and chalcogene diffusion fluxes. The relative concentration difference  $\Delta C$  due as a result of segregation can be estimated by comparison of the ‘‘concentration driving force,’’  $kT \nabla c / c$ , with other driving forces defined by Eq. (2), for example, with  $q \nabla I$ . Equating  $kT \nabla c / c \approx kT \Delta c / c \Delta x$  to  $q \nabla I \approx q I_m / \Delta x$  ( $\Delta x$  is the characteristic distance of the mass transfer), we have  $\Delta c / c \approx q I_m / kT$ . Thus, with  $q \approx 3 \times 10^{-30}$ ,  $kT \approx 4 \times 10^{-21}$  J, and  $I_m \approx 10^6$  W/m<sup>2</sup>, one obtains  $\Delta c / c \approx 10^{-3}$ . The coefficient  $D_x$  and  $s = D_x / D_z$  were used as fitting parameters for comparison of the theory with experiments.

For simplicity of numerical calculations, we assumed that the shape of the surface profile formed under illumination repeats the light intensity distribution [see Eq. (1)] and can be described by the formula

$$z(x, t) = h(t) \exp(-2x^2/w^2). \quad (12)$$

This is correct as the first approximation at initial stages of the profile evolution;  $h(t)$  gives the maximum height or depth of the profile as a function of exposure time.

Substituting Eq. (12) in Eq. (10), one can obtain an equation for  $h(t)$  in the form:

$$\frac{dh(t)}{dt} = Ah(t) + B. \quad (13)$$

Here  $A$  and  $B$  are coefficients, depending on the light intensity distribution and diffusion mobility, i.e., they depend on

the  $x$ -coordinate. The solution of Eq. (13) with the initial condition  $h(0) = h_0$  is

$$h(t) = -\frac{B}{A} + \frac{(Ah_0 + B) \exp(At)}{A}. \quad (14)$$

#### IV. COMPARISON WITH THE EXPERIMENT

Depending on the sign of the coefficients  $A$  and  $B$ ,  $h(t)$  will grow or decrease with time, i.e., will be positive or negative. Accordingly, the variation of the light intensity (with an appropriate set of parameters) results in inversion of the direction of the resultant diffusion flow (Fig. 3).

We start with the flat surface ( $h_0 = 0$ ) and see that at low intensities, such as  $I_m = 32$  W/cm<sup>2</sup>, we have a growth of hillock ( $h(t) > 0$ ); whereas with higher intensities ( $I_m = 320-1600$  W/cm<sup>2</sup>), we obtain dips ( $h(t) < 0$ ). The depths of these profiles measured at various intensities are shown by squares at the maximum times of the calculated curves (Fig. 3). The rate of the mass transfer essentially depends on the light intensity. As one can see from Figs. 2 and 3, the calculated values  $h(t)$  are in good agreement with the experimental data. The photo-induced diffusion coefficients calculated as  $D_x = \beta I$  from the kinetics of profile evolution varied in the range  $5 \times 10^{-13} - 5 \times 10^{-11}$  m<sup>2</sup>/s with  $32 < I_m < 3200$  W/cm<sup>2</sup>, and thus the average value of  $\beta = 1.5 \times 10^{-18}$  m<sup>4</sup>/J was obtained. The ratios  $D_x/D_z = s$  varied from 4 to 5 depending on the light intensity.

The threshold intensity (when  $h(t)$  changes its sign) depends on the parameters  $w$  and  $H$ , so that, using the same intensity, one can obtain hillocks instead of dips by variation of these parameters. Calculations show that the characteristic time of the profile variation also depends on  $w$  and  $H$ , increasing proportionally to  $w^3$  and  $H^{-1}$ .

Previously,<sup>13</sup> we analyzed the kinetics of patterning under periodic intensity distribution, typical for illumination by two crossing beams. We found good agreement between our calculations for  $h(t)$  and experimental data on SRG

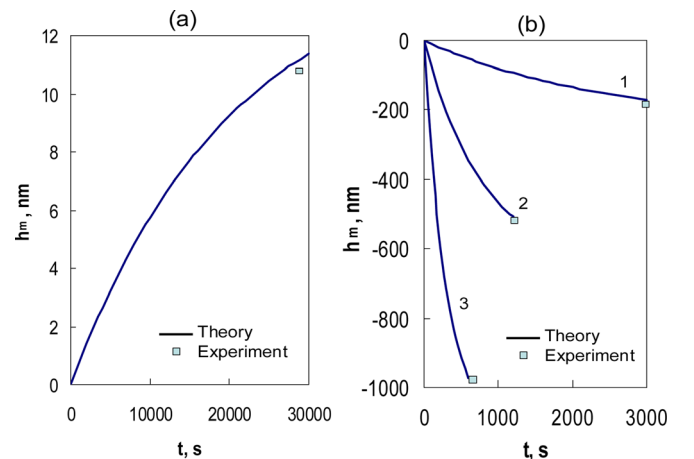


FIG. 3. (Color online) Formation of hillock (a), or dips (b) under illumination by Gaussian beams of low ( $I_m = 32$  W/cm<sup>2</sup>) and higher intensity, respectively (line 1,  $I_m = 320$  W/cm<sup>2</sup>; line 2,  $I_m = 800$  W/cm<sup>2</sup>; line 3,  $I_m = 1600$  W/cm<sup>2</sup>). Experimental values  $h(t)$  were obtained from the profiles similar to those in Fig. 1 under the constant product of  $I_m t$ . The calculations were made for  $w = 8 \mu\text{m}$  used in the experiments.

formation in  $\text{As}_2\text{S}_3$  films<sup>10</sup> (where valleys were formed in light fringes under high-enough intensities) and  $\text{As}_{0.3}\text{Se}_{0.7}$  films<sup>11</sup> (where the hills grew in the light fringes under much lower intensities). In both cases, we have obtained  $D_x I = \beta \approx 1.2 \times 10^{-20} \text{ m}^4/\text{J}$ , which is about two orders of magnitude smaller compared to  $\beta$  obtained from the growth of hillocks or dips under illumination by a focused Gaussian beam in the present experiments. This difference can be caused by different compositions and real structure of the films used in our case and in experiments on patterning kinetics under two-beam illumination.<sup>10,11</sup>

It is worth noting that dose-dependent formation of hillocks and dips in experiments with  $\text{As}_2\text{S}_3$  films,<sup>10</sup> illuminated by a focused beam, can be attributed to variation of the intensity rather than the dose. The threshold dose  $0.6 \text{ kJ/cm}^2$  in Ref. 10 with the exposure time of about 10 s corresponds to  $I \approx 60 \text{ W/cm}^2$ , which is close to our threshold intensity.

## V. CONCLUSIONS

Under assumptions that photo-induced evolution of the surface profiles occurs because of competition between the stress-induced atomic flux (toward irradiated regions of the film) and the diffusion flux induced by the increase of the bulk energy because of broken bonds (and directed from irradiated to dark regions), we have calculated the kinetics of the mass transfer in ChG films under illumination by a focused Gaussian beam. Depending on the light intensity, one can obtain either formation of hillocks or dips in the illuminated regions. The threshold intensity, which corresponds to the inversion of the mass transfer, depends on the beam waist  $w$  and on the film thickness  $H$ . The results of our calculations are confirmed by experiments on  $\text{As}_{0.2}\text{Se}_{0.8}$  glass films, illuminated by a focused Gaussian beam. From the comparison of experimental and theoretical profiles, the photo-induced diffusion coefficients  $D$  have been estimated

and found to be proportional to the light intensity  $I$  ( $D = \beta I$ ) with average  $\beta = 1.5 \times 10^{-18} \text{ m}^4/\text{J}$ .

## ACKNOWLEDGMENTS

This work is supported by Grant CK80126 of the Hungarian Scientific Research Fund and by the TAMOP 4.2.1./B-09/1/KONV-2010-007 project, which is co-financed by the European Union and European Social Fund.

- <sup>1</sup>S. R. Elliott, *J. Non-Cryst. Solids* **81**, 71 (1986).
- <sup>2</sup>D. K. Tagantsev and S. V. Nemilov, *Fiz. Khim. Stekla* **15**, 397 (1989).
- <sup>3</sup>H. Hisakuni and K. Tanaka, *Appl. Phys. Lett.* **65**, 2925 (1994).
- <sup>4</sup>H. Hisakuni and K. Tanaka, *Science* **270**, 975 (1995).
- <sup>5</sup>K. Tanaka and H. Hisakuni, *J. Non-Cryst. Solids* **198–200**, 714 (1996).
- <sup>6</sup>A. Ozols, O. Salminen, P. Riihola, and P. Monkkonen, *J. Appl. Phys.* **79**, 3397 (1996).
- <sup>7</sup>M. L. Trunov, *J. Phys. D: Appl. Phys.* **41**, 074011 (2008).
- <sup>8</sup>S. N. Yannopoulos and M. L. Trunov, *Phys. Status Solidi B* **246**, 1773 (2009).
- <sup>9</sup>D. Th. Kastrissios and S. N. Yannopoulos, *J. Non-Cryst. Solids* **299–302**, 935 (2002).
- <sup>10</sup>A. Salimonia, T. V. Galstian, and A. Villeneuve, *Phys. Rev. Lett.* **85**, 4112 (2000).
- <sup>11</sup>M. L. Trunov, P. M. Lytvyn, and O. M. Dyachyn'ska, *Appl. Phys. Lett.* **96**, 111908 (2010).
- <sup>12</sup>M. L. Trunov, P. M. Lytvyn, P. M. Nagy, and O. M. Dyachyn'ska, *Appl. Phys. Lett.* **97**, 031905 (2010).
- <sup>13</sup>Yu. Kaganovskii, D. L. Beke, and S. Kökényesi, *Appl. Phys. Lett.* **97**, 061906 (2010).
- <sup>14</sup>G. Martin, *Phys. Rev. B* **30**, 1424 (1984).
- <sup>15</sup>M. L. Trunov, P. M. Nagy, V. Takats, P. M. Lytvyn, S. Kokenyesi, and E. Kalman, *J. Non-Cryst. Solids* **355**, 1993 (2009).
- <sup>16</sup>H. Fritzsche, *Semiconductors* **32**, 850 (1998).
- <sup>17</sup>M. Kastner, D. Adler, and H. Fritzsche, *Phys. Rev. Lett.* **37**, 1504 (1976).
- <sup>18</sup>K. Shimikawa, N. Yoshida, A. Ganjoo, and Y. Kuzukawa, *Philos. Mag. Lett.* **77**, 153 (1998).
- <sup>19</sup>R. W. Boyd, *Nonlinear Optics* (Academic Press, Boston, 1992).
- <sup>20</sup>I. I. Shpak, Z. P. Gad'mashi, and I. I. Rosola, *Glass Phys. Chem.* **27**, 545 (2001).
- <sup>21</sup>K. Tanaka, N. Terakado, and A. Saitoh, *J. Optoelectron. Adv. Mater.* **10**, 124 (2008).